Applied Composite Materials
https://doi.org/10.1007/s10443-023-10153-5

The Influence of Processing Temperature on the Tensile Properties of Melt-Spun PLA Fibres and their Self-Reinforced Composites

Stergios Goutianos[1] · Justine Beauson[2]

Received: 15 February 2023 / Revised: 12 June 2023 / Accepted: 13 July 2023
© The Author(s) 2023

Abstract
The temperature during the consolidation of self-reinforced PLA composites has a significant effect on their mechanical properties. In the present work, the effect of the consolidation or processing temperature on the properties of melt-spun, highly oriented PLA fibres is experimentally studied through single fibre tests. It is shown that the Young's modulus and strain to failure of PLA fibres increases with exposure to consolidation / processing temperature, and the strength decreases more drastically. Using these data and findings from earlier studies, it is demonstrated that the dependence of the tensile properties of self-reinforced PLA composites on the processing temperature can be directly predicted from the single PLA fiber properties as a function of the processing temperature. This prediction holds true provided that the tensile properties of both the PLA fibers and self-reinforced PLA composites are measured using the same cross-head speed or strain rate.

Keywords Weibull distribution · Fibre strength · Poly(lactic acid) · PLA fibres · Self-reinforced composites

1 Introduction

As awareness for sustainable and environmentally friendly materials grows, bioplastics are gaining increasing interest. Polylactic acid (PLA), derived from renewable resources such as corn or sugar beets, is perhaps the most widely used bioplastic / biopolymer. It has relatively attractive mechanical properties compared to the other bioplastics, it is biodegradable and the industrial production capacity is high [1]. PLA, however, is primarily used as disposable or packaging material [2] due to its lower mechanical properties when compared to petro-based polymers.

✉ Stergios Goutianos
stergios.goutianos@ntnu.no

Justine Beauson
jube@dtu.dk

1 Department of Manufacturing and Civil Engineering, Norwegian University of Science and Technology, Gjøvik 2815, Norway

2 Department of Wind Energy, Technical University of Denmark, Roskilde 4000, Denmark

One way to improve the mechanical properties of neat PLA is to develop PLA composites by adding reinforcement such as cellulose in various forms [3–6]. The addition even of bio-based reinforcement does not, however, necessarily means that the environmental performance of these composites is equal to that of neat PLA i.e. the eco-performance of the composites may be lower [7–9].

An alternative approach is based on the concept of self-reinforced composites, where the matrix is reinforced with oriented fibres made from the same polymer but with a higher melting temperature [10–12]. The first self-reinforced composites were based on polyethylene [13] and later the concept was extended to various others material systems such as polypropylene [14–17], polyamide [18], aramid [19] and cellulose [20–22]. However, it is only recently that limited number of papers have applied this concept to develop self-reinforced PLA composites [9, 23–25] for fully biodegradable composites based on renewable resources.

The mechanical properties of self-reinforced composites can be enhanced by increasing the orientation of the polymer chains in the reinforcement [26] i.e. develop fibres of high stiffness and strength. Oriented PLA fibres produced by solution spinning can have very high properties, such as a tensile strength of 1 GPa [27] or 2.1 GPa with a Young's modulus of 16 GPa [28]. Commercial PLA fibres, however, are, typically produced by melt spinning to achieve higher production rates and to avoid the use of solvents [2]. Melt-spun PLA fibres have lower properties; the reported strength varies from 280 to 870 MPa and the Young's modulus from 5.2 to 9.2 GPa [2, 29–32]. The wide range of strength and modulus values reported originates from the strong dependence of the polymer fibre properties on: a) the PLA grade used, b) the extrusion process parameters, and c) the drawing parameters (Fig. 1a). Optimisation of the manufacturing parameters has been an active topic of research including PLA e.g. [2, 25, 27].

After the manufacturing of the fibers, the production of self-reinforced composites typically involves hot press-consolidation [9, 25]. This process involves heating of the materials to melt the PLA that will form the matrix but not the PLA fibres. However, during this process, the PLA fibres are also heated and their properties will be significantly changed. Therefore, the fibre properties that determine the properties of the self-reinforced PLA composites are in general quite different from the properties usually measured (after drawing but before composite processing). The aim of the present work is to study the influence of self-reinforced composite processing conditions on the PLA fibre properties and subsequently on the self-reinforced PLA composites.

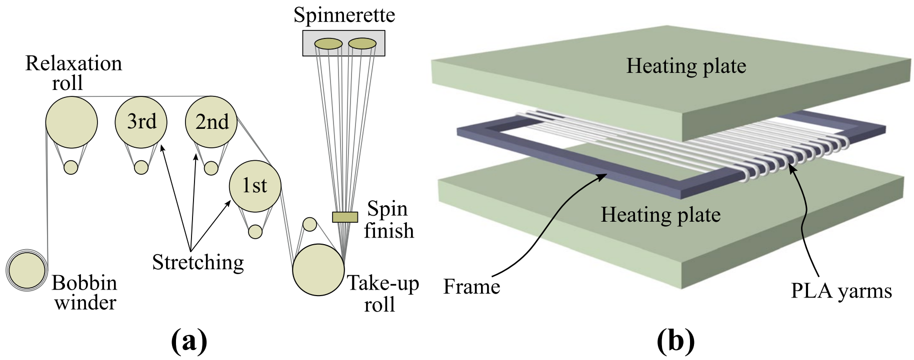

Fig. 1 Schematic of **a** solid-state drawing pilot line and **b** press-consolidation of the PLA yarns

The paper is structured as follows. First a statistical analysis of the fibre strength distribution is performed using various gauge lengths and testing speeds at room temperature. Then, the fibre properties are measured after subjecting them to different process temperatures at different testing speeds for a fixed gauge length. It should be emphasised that the draw ratio of the PLA fibres is kept constant. The results are then discussed in terms of their implications on composite properties. Lastly, the major findings are summarized.

2 Experimental Details

2.1 Materials

A high melting temperature and medium flow homopolymer PLA (L130 PLA grade) was purchased from Total Corbion PLA. The PLA material was first compounded and then melt spun into multi-fibre yarns (Fig. 1a) using a pilot line. The draw ratio was equal to 2.76. More details about the manufacturing process of the PLA yarns can be found elsewhere [33]. The focus of the current work is on the effect of the composite process parameters (to fabricate the self-reinforced PLA composites) on the PLA fibre properties and subsequently on the composite properties i.e. the starting point is after the PLA fibres have been melt-spun and drawn from the PLA compound.

After the PLA yarns were produced (Fig. 1a), the yarns were wound from the bobbins in a metal frame (see Fig. 1b) using a custom made winding machine. Subsequently, the frame was placed overnight in an oven under vacuum and temperature equal to 35 °C to dry the PLA fibres.

The PLA yarns were then press-consolidated in a custom-made press facility using a two-step process. In the first section of the press facility, the frame with the wound PLA yarns was heated for 10 min under vacuum to the process temperature, T_p. The heating was applied by the contact of two metal plates as shown in Fig. 1b). Subsequently, in the second step, the frame was quickly moved to the second section of the press facility and cooled down to 30 °C within 1 min under a pressure of 2 MPa. These process parameters are the same with the parameters used to manufacture self-reinforced PLA composites [25, 33, 34] and thus approximate the conditions that the PLA fibres experience during composite manufacturing. The process temperature, T_p, was varied from 155 °C to 180 °C in increments of 5 °C. In the process window from 155 °C to 175 °C, the PLA fibres do not melt, whereas at T_p = 180 °C the PLA fibres melt. It should be noted that in the present study there were fewer fibres in the frame compared to the case of composite manufacturing [25, 33, 34] and the pressure that the fibres experience may be less than 2 MPa. However, it can be argued that the potential difference in the applied pressure does not have a significant effect on the reported results.

2.2 Single Fibre Mechanical Testing

After press-consolidation, individual PLA fibres were carefully extracted from the PLA yarns to prevent any damage to the PLA fibres. For the different process temperatures, except the case of T_p = 180 °C, it was straightforward to extract single fibres. For the process temperature equal to 180 °C, only a limited number of fibres were extracted since at this temperature the fibres melt and stick to each other.

The single PLA fibre were tested in tension on a Favimat & Robot single fibre tester (Textechno H. Stein GmbH & Co. KG). Individual fibres were first loaded into a magazine (up to 25 samples) with a pretension weight of 100 mg attached to the bottom end of each fibre. Then, the robot moved one by one the fibres to the testing chamber. Each fiber was first clamped, and then a pretension ranging between 0.5 cN (for small gauge lengths) and 1.5 cN (for large gauge lengths) was applied. Subsequently, the linear density (mass per length) of the fiber was measured using a vibration method following the ASTM standard D1577-07 [35]. In this method, the resonance frequency was initially measured at a constant gauge length and pretension, allowing for the evaluation of the linear mass density. Following the linear density measurement, the fiber was subjected to tension testing. For all mechanical tests, a pretension of 0.1 cN was applied, and the load–displacement curves were recorded. By utilizing the linear density and the recorded loads, the fiber stress could be calculated.

The section of the paper that examines the fibre strength distribution, the fibres had not been press-consolidated and the gauge length was varied from 10 mm to 75 mm. Two sets of experiments were performed. In the first set, the cross-head speed was 20 mm/min for all gauge lengths. In the second set, the cross-head speed was varied, depending on the gauge length, to have a nominal strain rate, $\dot{\epsilon}$, equal to 0.25 s^{-1}. For each testing condition approximately 100 fibres were tested. These fibres were randomly selected from different bobbins to more accurately capture the variability in strength among the fibers.

For the investigation of the effect of the press-consolidation temperature on the mechanical properties of the fibres, the gauge length was constant and equal to 50 mm. The tests were performed at constant cross-head speed of 0.2, 20 and 200 mm/min for the different press-consolidation temperatures. In most cases, approximately 50 fibres were tested. All the fibres were taken from the same bobbin.

2.2.1 Fibre Strength Distribution

The fibre strength distribution, in particular of brittle fibres, is described by a Weibull distribution [36] and it can be typically a two or three-parameter distribution [37, 38]. By setting the threshold stress equal to zero, then the two parameter distribution, under uniform stress, is:

$$P_f(\sigma, L) = 1 - exp\left(-\frac{L}{L_o}\left(\frac{\sigma}{\sigma_o}\right)^m\right) \tag{1}$$

where the P_f is the probability of failure of a fibre of length L at stress σ. The characteristic length is denoted as L_o. The Weibull modulus is m and the characteristic strength is σ_o.

To experimentally determine m and σ_o, Eq. 1, with L_o set equal to L, is re-written as:

$$\ln\left(\ln\frac{1}{1 - P_f(\sigma, L)}\right) = m\ln\sigma - m\ln\sigma_o \tag{2}$$

Then, the experimental data are fit with a straight line in a $\ln\sigma$ – $\ln\left(\ln 1/(1 - P_f(\sigma, L))\right)$ plot. From the coefficients of the straight line, the Weibull parameters can be determined [39]. Then, from m and σ_o, the mean fibre strength, σ_m, can calculated from:

$$\left(\frac{\sigma_m}{\sigma_o}\right) = \left(\frac{L}{L_o}\right)^{-1/m}\Gamma\left(1 + \frac{1}{m}\right) \tag{3}$$

where Γ is the gamma function. The probability of failure of the ith fibre, P_{f_i}, in Eq. 1 is calculated by:

$$P_{f_i} = \frac{i}{N+1} \tag{4}$$

where N is the total number of successfully tested fibers for the specific testing conditions. Prior to applying Eq. 4, the fibres are sorted from lowest to highest strength. After sorting the fibres, the median strength, σ_M, can be also calculated. A number of other probability estimators than Eq. 4 have been proposed [40, 41]. Some estimators are less biased than others [40, 42, 43], however, for the purposes of the present study Eq. 4 is sufficient for determining the Weibull parameters of the PLA fibers.

In addition to utilizing the Weibull distribution, the fibre strength is also characterized by a Gaussian distribution. A Weibull distribution mainly applies to brittle materials, whereas for ductile materials such as the PLA fibres, used in the present study, a Gaussian or normal distribution can be used.

2.3 Thermal Analysis

Temperature-modulated Differential Scanning Calorimetry (DSC) (DSC 214 Polyma, NETZSCH-Gerätebau GmbH) was used to measure the thermal transitions of the PLA fibres. The samples, of approximately 10 mg, were heated from 25 °C to 200 °C with a heating rate of 5 °C/min, an amplitude of 0.8 °C/min and a period of 60s, using N_2 as purging gas.

The crystallinity $X_c(\%)$ of the PLA fibres was calculated by:

$$X_c(\%) = \frac{\Delta H_M - \Delta H_c}{\Delta H_{100}} 100 \tag{5}$$

where ΔH_M represents the melting enthalpy and ΔH_c is the cold crystallization enthalpy which was assumed to be zero as no cold crystallization was observed in the measurements. ΔH_{100} is the melting enthalpy of 100% crystalline PLA and is set equal to 93.0J/g based on previous studies [44, 45].

3 Results

3.1 Weibull Analysis

Figure 2 shows the Weibull plots for two different gauge lengths, L, equal to 15 and 25 mm, respectively. For each gauge length two sets of data are presented, one obtained under constant a cross-head speed and the other obtained under a constant nominal strain rate. From such plots for all gauge lengths, the data for Tables 1 and 2 are obtained.

Table 1 shows the Weibull parameters for the PLA fibres tested at a constant cross-head speed, u, equal to 20 mm/min and independent of the gauge length, L, i.e. for higher gauge lengths, the strain rate is lower. The median strength, σ_M, is the strength of the median fibre after the fibres are sorted as described in Sect. 2.2.1. It can be seen that the difference between the median strength and the average strength, σ_{av}, ranges from approximately 3.3% for L = 75 mm and 0.4% for L = 15 mm. The characteristic strength, σ_o, is higher

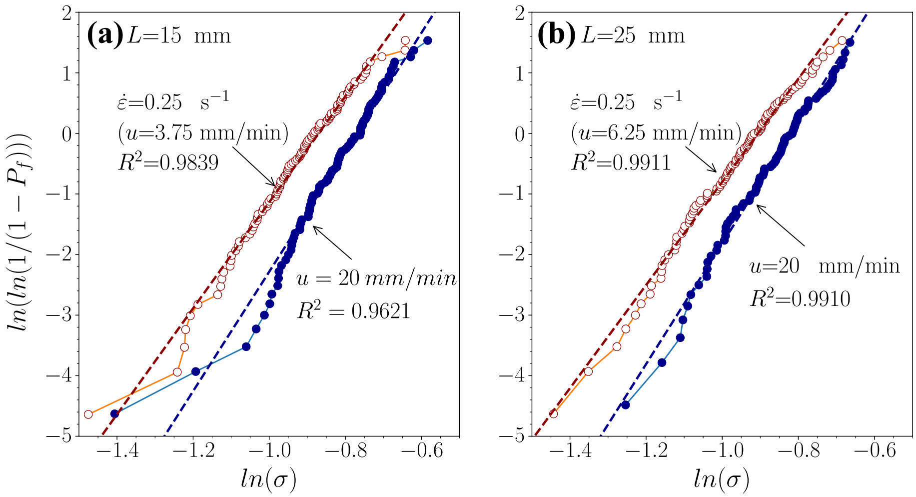

Fig. 2 Weibull plots for u = 20 mm/min and $\dot{\epsilon}$ = 0.25 s^{-1} for **a** gauge length equal to 15 mm and **b** gauge length equal to 25 mm

than σ_M or σ_{av} for all gauge lengths. The biggest difference of about 6% is obtained for L = 10 mm. The lowest Weibull modulus, m, is 7.2 and obtained for L = 10 mm. For all gauge lengths, the Weibull modulus is large and secondly there is one to one correspondence with the standard deviation of the Gaussian distribution. The smallest standard deviation is for L = 60 mm, for this gauge length, the largest Weibull modulus was measured.

Table 2 is similar to Table 1 with the difference that for each gauge length, the cross-head displacement is adjusted to achieve a nominal strain rate, $\dot{\epsilon}$ equal to 0.25 s^{-1} i.e. $u = \dot{\epsilon}\, L$. It can be seen that the variation of the Weibull modulus and of the standard deviation are smaller compared to Table 1. The median strength is approximately equal to the average strength; the difference is less than 1% except for the case of L = 50 mm with a 3% difference. As in Table 1, the characteristic strength is higher than the median and average strengths; the difference is about 5% for all tested gauge lengths.

Table 1 Tensile strength of melt-spun PLA fibres after drawing as function of the gauge length. Tension under constant cross-head speed, u = 20 mm/min

Gauge Length L (mm)	No N (-)	Weibull Modulus m (-)	Char Strength σ_o (MPa)	Mean Strength σ_m (MPa)	Median Strength σ_M (MPa)	Average Strength σ_{av} (MPa)	St. Dev. $\pm$ (MPa)
10	103	7.20	487.64	456.82	468.82	456.76	66.92
15	102	9.87	463.74	440.91	442.81	441.14	49.75
25	88	9.96	441.44	419.90	426.36	420.33	49.07
40	98	8.21	412.95	389.38	396.19	389.72	54.01
50	103	8.57	402.41	380.21	383.58	381.68	53.54
60	101	11.28	402.14	384.47	382.24	384.77	39.80
75	102	8.17	392.98	370.46	383.64	370.73	51.13

Table 2 Tensile strength of melt-spun PLA fibres after drawing as function of the gauge length. Tension under constant nominal strain rate, $\dot{\varepsilon} = 0.25\ \mathrm{s}^{-1}$

Gauge Length	No	Weibull Modulus	Char Strength	Mean Strength	Median Strength	Average Strength	St. Dev.
L	N	m	σ_o	σ_m	σ_M	σ_{av}	±
(mm)	(-)	(-)	(MPa)	(MPa)	(MPa)	(MPa)	(MPa)
10	98	9.25	436.84	419.19	410.40	414.52	51.48
15	103	8.75	418.90	396.18	399.24	396.50	52.36
25	102	8.51	404.20	381.78	385.20	382.14	52.33
40	91	7.81	392.83	369.52	371.72	369.89	54.31
50	110	8.64	389.07	367.74	379.34	367.97	48.57
60	104	8.25	375.45	354.11	361.44	354.39	49.00
75	99	9.91	376.36	358.01	358.80	358.33	42.43

A more accurate estimation of the Weibull modulus can be obtained by the linear fit of the median stress (from Tables 1 and 2) as a function of the gauge length (see Fig. 3). The Weibull modulus for the fibres tested at a constant cross-head speed is 9.3, whereas for the the fibres tested at a constant nominal strain rate, the Weibul modulus is found to be 15.5.

Figure 4 summarises the Young's modulus and failure strain of the melt-spun PLA fibres after drawing as a function of the gauge length. As expected the Young's modulus is independent of the gauge length and approximately equal to 7.37 GPa (for $u = 20$ mm/min or $\dot{\varepsilon} = 0.25\ \mathrm{s}^{-1}$). The failure strain increases with the gauge length. However, the dependence of the failure strain to the gauge length is weak. As can be seen the in Fig. 4b, the average failure strain is approximately 33.8% for $L = 10$ mm and 29.1% for $L = 75$ mm.

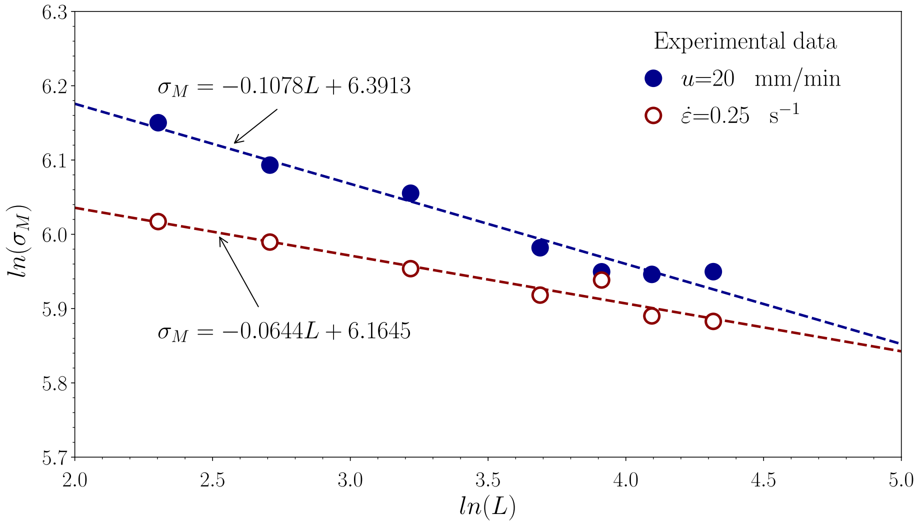

Fig. 3 Logarithmic plot of the median stress of melt-spun PLA fibres after drawing, tested at constant cross-head speed and nominal strain, as a function of the gauge length (see Tables 1 and 2). The slope of the straight line is $-1/m$

3.2 Effect of Processing Temperature on Thermal Properties and Crystallinity

Figure 5 displays typical examples of the DSC curves for melt-spun, drawn PLA fibres before and after press-consolidation, under a process temperature, T_p. The DSC results of the effect of the process temperature are summarized in Table 3. It can be seen that the onset temperature, melting temperature and the crystallinity level are all gradually increase as the process temperature, T_p, rises. The rate of increase is significantly higher as T_p approaches a temperature equal to 175 °C. Beyond this characteristic temperature, the onset temperature, melting temperature and the crystallinity level drop substantially due the melting of the PLA fibres during processing as it is clear from Table 3.

3.3 Effect of Processing Temperature on Mechanical Properties

The effect of the processing temperature, T_p, is graphically illustrated in Fig. 6 for the fibre's Young's modulus, in Fig. 7 for the fibre strength, and in Fig. 8 for fibre failure strain. In these graphs, each symbol represents the average value obtained from several tests (see Table 4). The results for the Young's modulus, strength and failure strain are also tabulated in Tables 5, 6, and 7, respectively, allowing for a clearer observation of the standard deviation as well.

It can be seen that the Young's modulus of the PLA fibres increases with the processing temperature and the maximum value is obtained for T_p between 160–165 °C, an increase of approximately 10% with respect to the fibres without processing. Higher processing temperatures result in lower Young's modulus and a T_p equal to 180 °C (higher than the fibre melting temperature) gives an E_f equal to 3.62 GPa (for u = 2 mm/min) which is approximately equal to the Young's modulus of the PLA material (see Sect. 2.1) without any drawing. The effect of the processing temperature is stronger on the fibre strength. A process temperature of 165 °C results in a fibre strength reduction by 1/3, whereas when T_p is 175 °C the fibre strength is reduced b a factor of 2. The failure strain of the fibres (Fig. 8 and Table 7) increases with increasing the process temperature up to T_p equal to 175 °C. It is interesting to observe that the PLA fibre

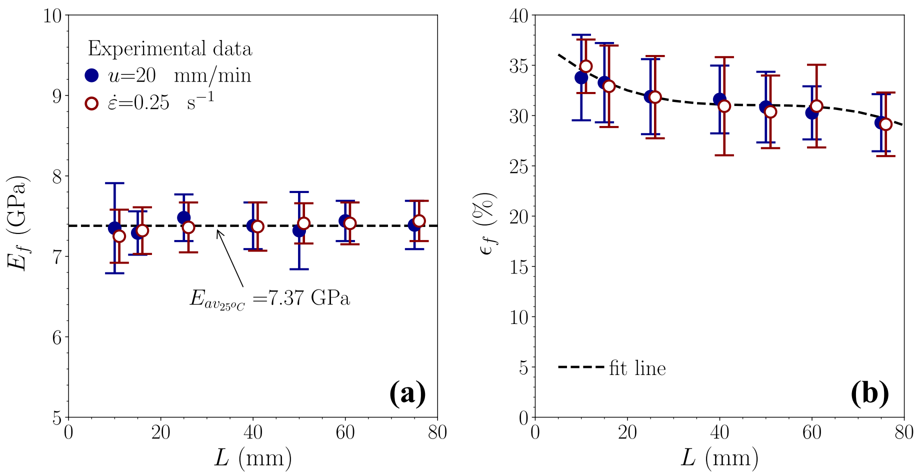

Fig. 4 Young's modulus and failure strain of melt-spun PLA fibres after drawing tested under constant cross-head speed and constant nominal strain rate. The error bars are based on standard deviation

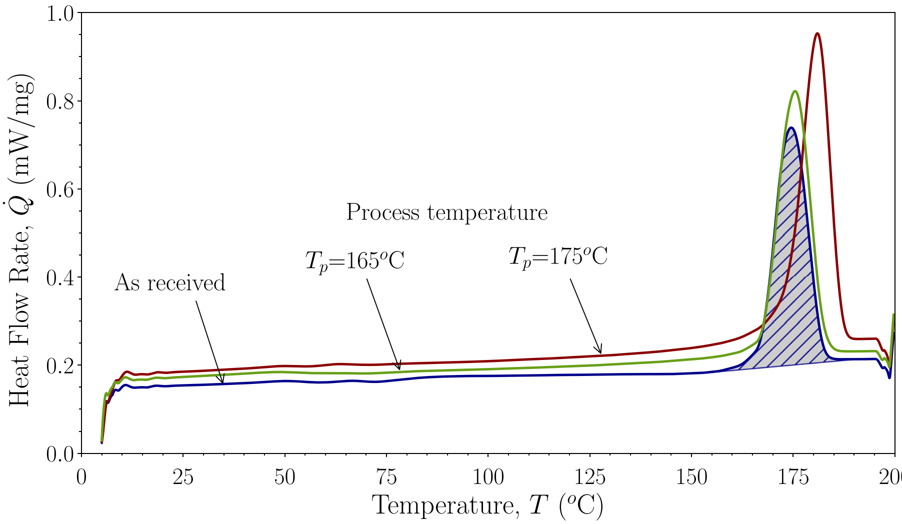

Fig. 5 Typical DSC curves of a melt-spun and drawn PLA fibre and of PLA fibres post processed at T_p equal to 165 °C and 175 °C, respectively

failure strain is nearly 2 times higher than the fibres which have not been subjected to a post process after drawing.

From the results presented above, a strong effect of the cross-head speed can be observed for all the characteristic mechanical properties (Young's modulus, strength and failure strain) even if the cross head speed increases from 2 to 20 mm/min. The importance of this will be discussed in the next Section.

4 Discussion

4.1 Prediction of UD Composite Properties

It is possible to use the results presented in the previous Section to predict the mechanical properties of unidirectional self-reinforced PLA composites. In Sect. 3.1 it was

Table 3 Thermal properties and crystallinity of the PLA fibres as a function of the processing temperature

Process Temperature (°C)	Onset Temperature (°C)	St Dev ±	Melting Temperature (°C)	St Dev ±	Crystallinity (%)	St. Dev. ±
25	167.10	0.17	174.47	0.25	65.48	0.64
155	167.17	0.06	174.87	1.16	67.31	1.63
160	167.45	0.07	174.85	0.21	67.89	2.39
165	167.93	0.15	175.77	0.25	70.81	1.43
170	167.90	0.40	175.73	0.25	70.67	1.75
175	173.50	0.10	180.73	0.31	79.43	2.40
180	165.97	0.29	174.10	0.36	66.93	3.34

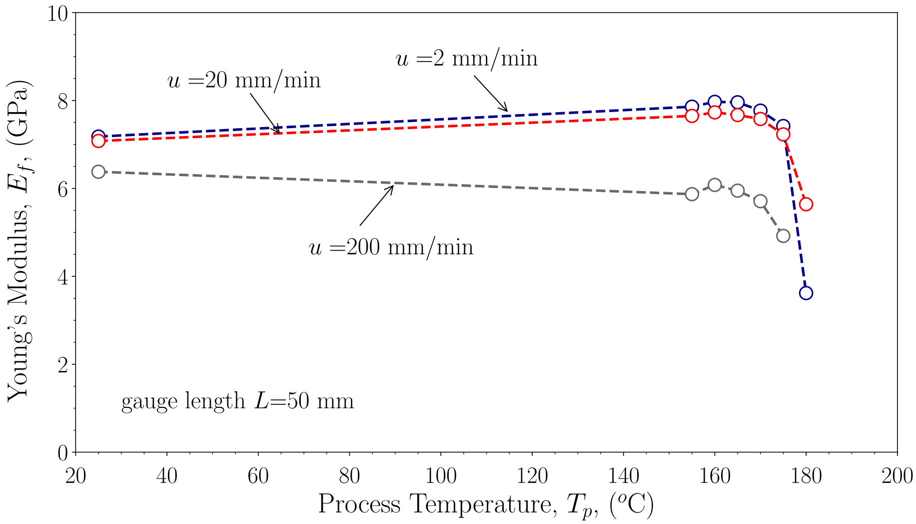

Fig. 6 Effect of processing temperature, T_p, and cross-head speed, u, on the PLA fibre Young's modulus, E_f. The gauge length, L, is 50 mm

shown, as it should be expected, that the failure of the highly oriented PLA fibres does not depend on defects. Then, the average stress–strain curve (based on engineering stress and strain) of the PLA fibres can be obtained as the average of the individual single fibre tests as shown in Fig. 9. Figure 9 refers to fibres tested with u equal to 20 mm/min and the fibres have not been processed after drawing. As can be seen from Table 4, 45 fibres are used to calculate the average PLA fibre stress–strain curve. As the applied displacement increases, the average stress–strain curve is based on a

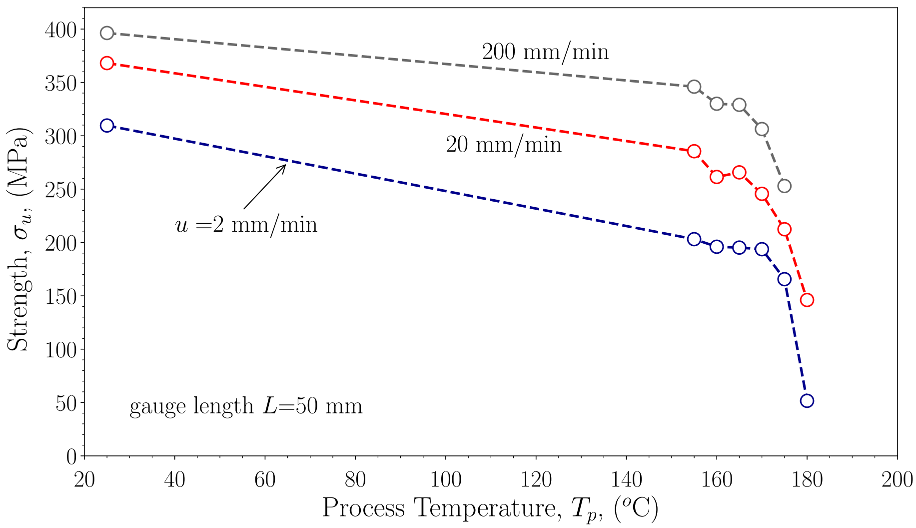

Fig. 7 Effect of processing temperature, T_p, and cross-head speed, u, on the PLA fibre strength, σ_u. The gauge length, L, is 50 mm

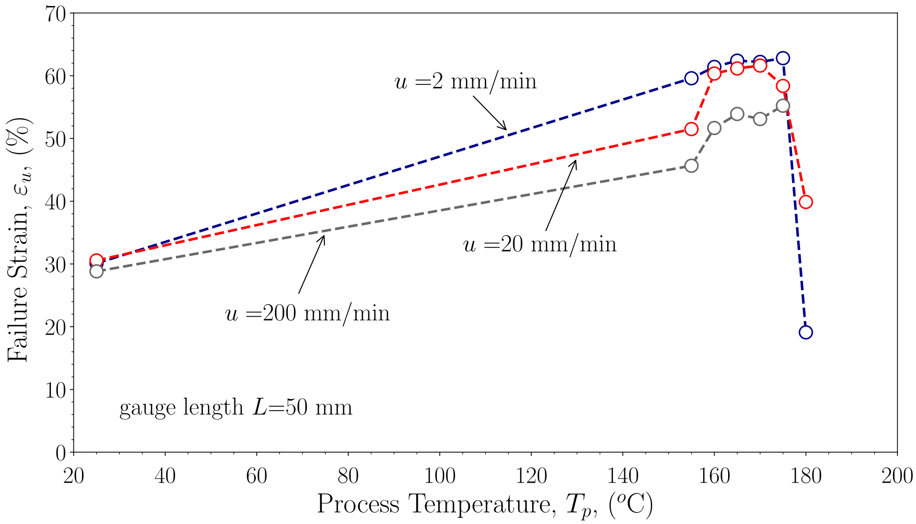

Fig. 8 Effect of processing temperature, T_p, and cross-head speed, u, on the PLA fibre strength, ε_u. The gauge length, L, is 50 mm

continuous decreased number of single fibre tests, since some fibres break earlier than the other fibres.

The procedure described in Fig. 9 is repeated for the different processing temperatures, T_p, and the results are plotted in Fig. 10. It can be clearly seen that the average PLA fibre stress–strain curves for fibres that have been thermally processed are significantly different from the average PLA fibre stress–strain curve after drawing. More importantly the average PLA fibre stress–strain curves are remarkably qualitatively similar with the stress–strain curves of unidirectional PLA self-reinforced composites [34].

Using the linear part of the average PLA fibre stress–strain curves or the results from Table 5, the Young's modulus of the self-reinforced composites is predicted using the rules of mixtures and compared with experimental measurements [34]. It should be noted, that in the experiments reported in Ref. [34], the fibre volume fraction was 50%. Therefore, in the rule of mixtures, the fibre volume fraction is assumed to be equal to 50% and the modulus of the PLA matrix is equal to 3.62 (Table 5 - T_p = 180 °C). The predictions are

Table 4 Number of PLA fibre tested in tension at different process temperatures and constant cross-head testing speeds. The gauge length, L, is 50 mm

Process Temperature (°C)	u = 2 mm/min No (-)	u = 20 mm/min No (-)	u = 200 mm/min No (-)
25	46	45	39
155	41	45	44
160	42	60	47
165	44	63	45
170	51	42	47
175	49	49	60
180	5	5	-

Table 5 PLA fibre Young's modulus as function of process temperature. Tension under constant cross-head speed. The gauge length, L, is 50 mm

Process	$u = 2$ mm/min		$u = 20$ mm/min		$u = 200$ mm/min	
Temperature	Young's modulus		Young's modulus		Young's modulus	
(°C)	(GPa)	±	(*GPa*)	±	(GPa)	±
25	7.18	0.28	7.08	0.34	6.38	0.36
155	7.86	0.31	7.65	0.36	5.87	0.47
160	7.97	0.59	7.73	0.26	6.08	0.35
165	7.96	0.40	7.67	0.43	5.95	0.47
170	7.77	0.48	7.58	0.26	5.71	0.48
175	7.42	0.65	7.23	0.48	4.92	0.94
180	3.62	0.32	5.64	0.63	-	-

Table 6 PLA tensile fibre strength as function of process temperature. Tension under constant cross-head speed. The gauge length, L, is 50 mm

Process	$u = 2$ mm/min		$u = 20$ mm/min		$u = 200$ mm/min	
Temperature	Strength		Strength		Strength	
(°C)	(MPa)	±	(MPa)	±	(MPa)	±
25	309.6	41.9	368.1	47.6	396.3	73.0
155	203.1	19.5	285.5	37.5	346.0	41.7
160	196.0	31.0	261.4	26.9	330.0	37.7
165	195.2	26.6	265.7	19.1	329.0	35.2
170	193.7	27.7	245.6	33.1	306.3	35.7
175	165.6	22.6	212.4	30.6	252.9	44.9
180	51.6	19.4	146.1	37.0	-	-

Table 7 PLA tensile fibre failure strain as function of process temperature. Tension under constant cross-head speed. The gauge length, L, is 50 mm

Process	$u = 2$ mm/min		$u = 20$ mm/min		$u = 200$ mm/min	
Temperature	Failure strain		Failure strain		Failure strain	
(°C)	(%)	±	(%)	±	(%)	±
25	30.1	4.0	30.6	3.8	28.8	4.8
155	59.6	12.5	51.5	9.4	45.6	9.2
160	61.4	16.8	60.4	7.3	51.7	6.3
165	62.4	16.2	61.2	8.7	53.9	10.3
170	62.2	17.1	61.6	10.1	53.1	8.8
175	62.8	13.0	58.4	15.4	52.2	12.6
180	19.1	8.2	39.9	10.5	-	-

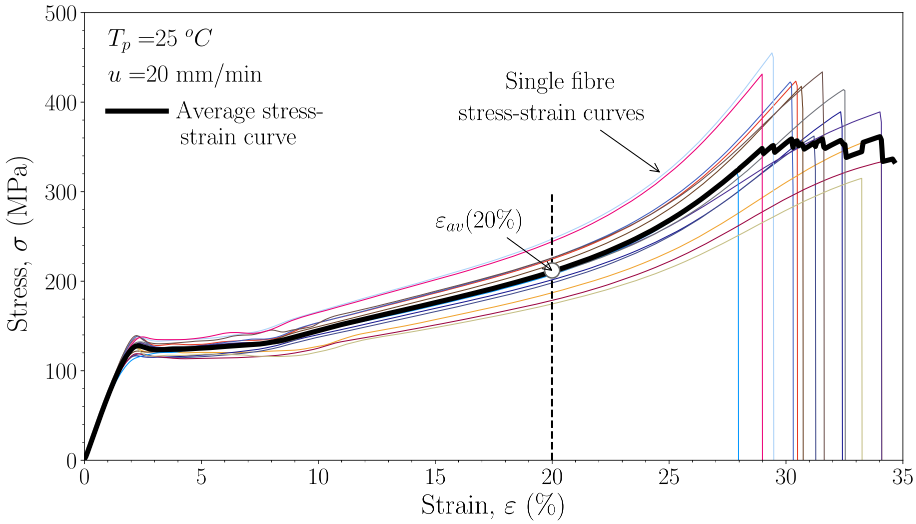

Fig. 9 Average PLA fibre stress–strain curve from individual single fibre tests. The gauge length, L, is 50 mm and the cross-head speed, u, is 20 mm/min

given in Table 8. It can be seen that the predictions are in agreement with the measurements. Therefore, it is clear that one should not use the fibre properties after drawing (e.g. ignoring the changes that occurs during manufacturing or processing of the composites) to predict or understand the behaviour of the PLA self-reinforced composites.

In a similar fashion, the strength of unidirectional composites is predicted by utilizing the results of Fig. 10 as a function of T_p and compared with experiments in Table 9. As mentioned before, it is assumed that the fibre volume fraction is 50%. Additionally,

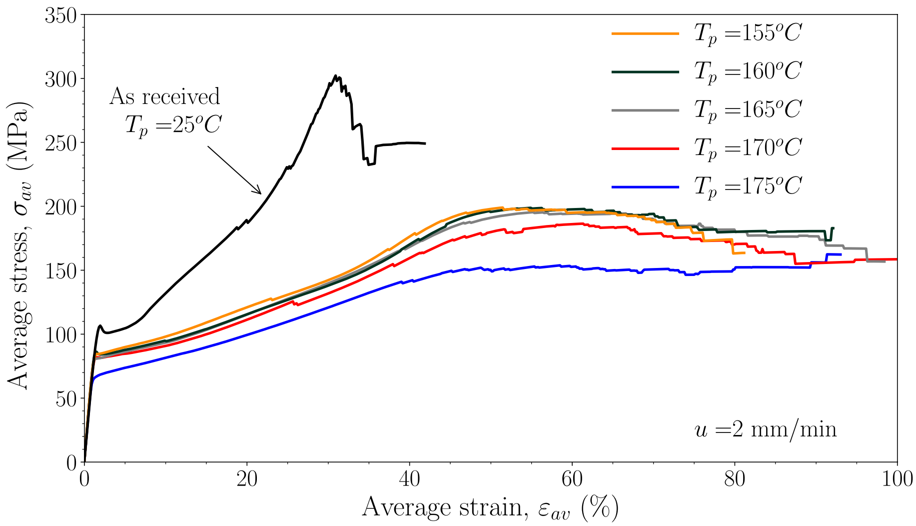

Fig. 10 Average PLA fibre stress–strain curves for different processing temperatures, T_p. The gauge length, L, is 50 mm and the cross-head speed, u, is 2 mm/min

Table 8 Predicted UD composite Young's modulus from single fibre experiments as a function of the processing temperature

	From single fibre tests		Composite tests	
Process	Young's Modulus		Young's Modulus	
Temperature	Average		Average	
(°C)	(GPa)	±	(GPa)	±
155	5.74	0.32	5.90	0.20
160	5.80	0.47	5.70	0.20
165	5.79	0.36	5.80	0.20
170	5.70	0.41	5.80	0.10

based on earlier findings [33], the PLA matrix fails early in a brittle manner at low applied strains and therefore the strength of the composites primarily depends on the PLA fibers. Consequently, the strength of the unidirectional fibre composites can be estimated by multiplying the maximum stress from Fig. 10 with 0.5 (fibre volume fraction). As can be seen from Table 9, the predictions agree with the experiments taking into account uncertainties in the fibre volume fraction, process temperature (T_p), and variations in the manufacturing of the PLA fibres (melt spinning and drawing).

Similar strength predictions could be obtained if the fibre strength were taken from Table 6, however, this approach is less rigorous. This becomes evident when considering the failure strain. The failure strain from Table 6 is in the order of 60% for T_p in the range of 155–175 °C. Beauson et al. [34] found that the failure strain, for similar T_p, ranges between 90 and 150%. The failure strain from Fig. 10 is between 90 and 100% and closer to the experimental measurement. One should expect that increasing the number of fibres tested (Table 4) would lead to better agreement with the experiments since the failure strain depends in the single PLA fibres with the higher strain-to-failure.

Quite often single fibre testing or in particular yarn testing is performed at relatively high cross-head speeds, between 100 to 500 mm/min. On the other hand, composites are tested at lower speed in the order of 1 to 5 mm/min. Figure 11 shows the average fibre stress–strain curve after drawing and after processing at 165 °C for three different cross head speeds (2, 20, and 200 mm/min). As can be clearly seen the effect of the cross-head speed is significant. If the case of the fibre processed at 165 °C is considered, following the method presented above, the predicted composite strength is 149.8 MPa when u is 200 mm/min. This value is significantly higher than the experimental

Table 9 Predicted UD composite strength from single fibre experiments as a function of the processing temperature

	From single fibre tests		Composite tests	
Process	Strength		Strength	
Temperature	Average		Average	
(°C)	(MPa)	±	(MPa)	±
155	99.5	13.6	113.3	3.0
160	99.4	15.9	100.0	1.0
165	97.7	16.2	93.0	3.0
170	93.2	18.4	84.0	7.0

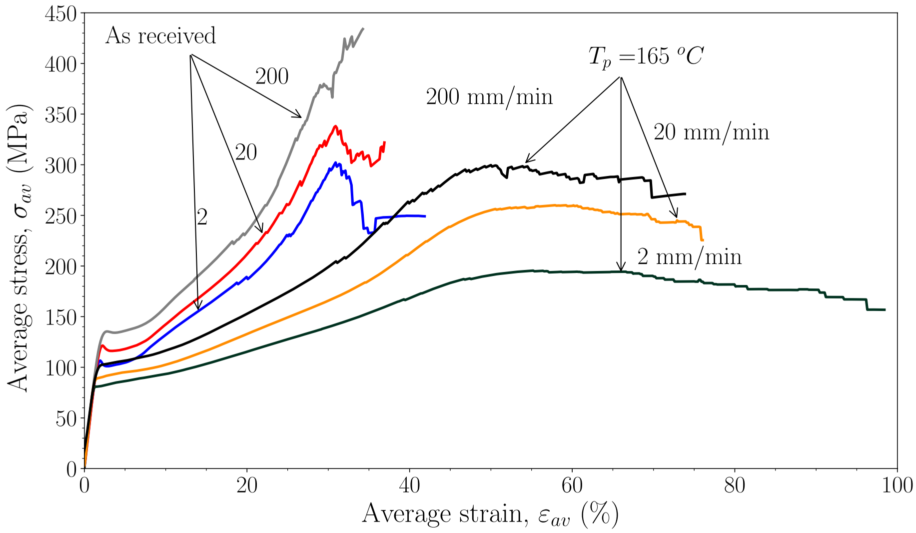

Fig. 11 Effect of testing speed on the average PLA fibre stress–strain curves after drawing and after processing at T_p equal to 165 °C. The gauge length, L, is 50 mm

measurement (93 MPa, Table 9) or the predicted value using u equal to 2 mm/min (97.7 MPa, Table 9). Thus, it is advantageous to test the polymer fibres at low speeds, corresponding to speeds used in composite testing, in order to directly predict the composite behaviour without performing experiments at the composite level.

4.2 Fibre Properties as Function of the Processing Temperature

The processing temperature, T_p, is higher than the glass transition temperature, T_p, of PLA, which is in the order of 60 °C. The heat treatment or annealing can promote various simultaneous microstructural effects, including polymer chain relaxation, orientation, and crystallization (Table 3), which in turn significantly impact the mechanical properties of the oriented PLA fibres themselves as shown in Sect. 3.3 and their self-reinforced composite properties (Sect. 4.1). An in-depth understanding of the interplay between these microstructural changes would require modelling at the molecular level which is beyond the scope of the current work. Here, it should be emphasised that increasing the processing temperature results in an increase of the Young's modulus and strain to failure (increased deformation) but at the same time the fibre strength decreases more drastically.

5 Concluding Remarks

The effect of the processing temperature on the mechanical properties of melt-spun oriented PLA fibres was examined through single fibre tests. It was shown that increasing the processing temperature increases the Young's modulus and strain to failure of the PLA fibres but at the same time it decreases strength at higher rate their. After a certain processing temperature, the PLA fibres melt completely and their properties reduce to those of amorphous PLA. It was also shown, that once the properties of the oriented PLA fibres are known, it is possible to predict the tensile properties of the unidirectional PLA self-reinforced composites. This prediction requires that the fiber properties account for the influence of the processing temperature, and that both the fibers and composites are tested at a similar strain rate.

Funding Open access funding provided by NTNU Norwegian University of Science and Technology (incl St. Olavs Hospital - Trondheim University Hospital). The work has received funding from the European Unions Horizon 2020 Research and Innovation Programme under Grant Agreement No 685614 (BIO4SELF).

Data Availability The datasets generated during and/or analysed during the current study are available from the corresponding author on reasonable request.

Declarations

Conflict of Interest The authors declare no competing interests.

Open Access This article is licensed under a Creative Commons Attribution 4.0 International License, which permits use, sharing, adaptation, distribution and reproduction in any medium or format, as long as you give appropriate credit to the original author(s) and the source, provide a link to the Creative Commons licence, and indicate if changes were made. The images or other third party material in this article are included in the article's Creative Commons licence, unless indicated otherwise in a credit line to the material. If material is not included in the article's Creative Commons licence and your intended use is not permitted by statutory regulation or exceeds the permitted use, you will need to obtain permission directly from the copyright holder. To view a copy of this licence, visit http://creativecommons.org/licenses/by/4.0/.

References

1. Auras, R., Harte, B., Selke, S.: An overview of polylactides as packaging materials. Macromol. Biosci. **4**, 835–864 (2004)
2. Mai, F., Wei, T., Bilotti, E., Peijs, T.: The influence of solid-state drawing on mechanical properties and hydrolytic degradation of Melt-Spun Poly(Lactic Acid) (PLA) Tapes. Fibers. **3**, 523–538 (2015)
3. Oksman, K., Skrifvars, M., Selin, J.-F.: Natural fibres as reinforcement in polylactic acid (PLA) composites. Compos. Sci. Technol. **63**, 1317–1324 (2003)
4. Graupner, N., Herrmann, A.S., Müssig, J.: Natural and man-made cellulose fibre-reinforced poly(lactic acid) (PLA) composites: an overview about mechanical characteristics and application areas. Composites: Part A. **40**, 810–821 (2009)
5. Berglund, L.A., Peijs, T.: Cellulose biocomposites-from bulk moldings to nanostructured systems. MRS Bull. **35**, 201–207 (2010)
6. Blaker, J.J., Lee, K.-Y., Walters, M., Drouet, M., Bismarck, A.: Aligned unidirectional PLA/bacterial cellulose nanocomposite fibre reinforced PDLLA composites. React. Funct. Polym. **85**, 185–192 (2014)
7. Cabrera, N.O., Alcock, B., Loos, J., Peijs, T.: Processing of all-polypropylene composites for ultimate recyclability. Institution of Mechanical Engineers Part L- Journal of Materials-Design and Applications. **2**, 145–155 (2004)
8. Goutianos, S., Peijs, T., Nystrom, B., Skrifvars, M.: Development of flax based textile reinforcements for composite applications. Appl. Compos. Mater. **13**, 199–215 (2006)
9. Mai, F., Tu, W., Bilotti, E., Peijs, T.: Preparation and properties of self-reinforced poly(lactic acid) composites based on oriented tapes. Composites: Part A. **76**, 145–153 (2015)
10. Hine, P., Ward, I., Olley, R., Bassett, D.: The hot compaction of high modulus meltspun polyethylene fibres. J. Mater. Sci. **28**, 316–324 (1993)
11. Loos, J., Schimanski, T., Hofman, J., Peijs, T., Lemstra, P.J.: Morphological investigations of polypropylene single-fibre reinforced polypropylene model composites. Polymer **42**(42), 3827–3834 (2001)

12. Alcock, B., Peijs, T.: Technology and development of self-reinforced polymer composites. In: Abe, A., Kausch, H.H., Moller, M., Pasch, H. (eds.) Advances in Polymer Science, vol. 251, pp. 1–76. Springer-Verlag, Berlin, Berlin, Germany (2013)
13. Capiati, N.J., Porter, R.S.: The concept of one polymer composites modelled with high density polyethylene. J. Mater. Sci. **10**, 1671–1677 (1975)
14. Hine, P.J., Ward, I.M., Jordan, N.D., Olley, R., Bassett, D.C.: The hot compaction behaviour of woven oriented polypropylene fibres and tapes. I. Mechanical properties. Polymer. **44**, 1117–1131 (2003)
15. Ward, I., Hine, P.: The science and technology of hot compaction. Polymer **45**, 1413–1427 (2004)
16. Cabrera, N.O., Alcock, B., Klompen, E.T.J., Peijs, T.: Filament winding of co-extruded polypropylene tapes for fully recyclable all-polypropylene composite products. Appl. Compos. Mater. **15**, 27–45 (2008)
17. Cabrera, N.O., Reynolds, C.T., Alcock, B., Peijs, T.: Non-isothermal stamp forming of continuous tape reinforced all-polypropylene composite sheet. Compos. A **39**, 1455–1466 (2008)
18. Barkoula, N.M., Peijs, T., Schimanski, T., Loos, J.: Processing of single polymer composites using the concept of constrained fibers. Polym. Compos. **26**, 114–120 (2005)
19. Zhang, J.M., Mousavi, Z., Soykeabkaew, N., Smith, P., Nishino, T., Peijs, T.: All-aramid composites by partial fiber dissolution. ACS Appl. Mater. Interfaces **2**, 919–926 (2010)
20. Nishino, T., Matsuda, I., Hirao, K.: All-cellulose composite. Macromolecules **37**, 7683–7687 (2004)
21. Qin, C., Soykeabkaew, N., Xiuyuan, N., Peijs, T.: The effect of fibre volume fraction and mercerization on the properties of all-cellulose composites. Carbohyd. Polym. **71**, 458–467 (2008)
22. Goutianos, S., Arévalo, R., Sørensen, B.F., Peijs, T.: Effect of processing conditions on fracture resistance and cohesive laws of binderfree all-cellulose composites. Appl. Compos. Mater. **21**, 805–825 (2014)
23. Jia, W., Gong, R.H., Hogg, P.J.: Poly(lactic acid) fibre reinforced biodegradable composites. Compos. B **62**, 104–112 (2014)
24. Li, R., Yao, D.: Preparation of single poly(lactic acid) composites. J. Appl. Polym. Sci. **107**, 2909–2916 (2008)
25. Buyle, G., Van Der Schueren, L., Beauson, J., Goutianos, S., Schillani, G., Madsen, B.: Self-reinforced biobased composites based on high stiffness PLA yarns. IOP Conf. Ser.: Mater. Sci. Eng. **406**, 012038 (2018)
26. Smith, P., Lemstra, P.J.: Ultra-high-strength polyethylene filaments by solution spinning/drawing. J. Mater. Sci. **15**, 505–514 (1980)
27. Penning, J., Dijkstra, H., Pennings, A.: Preparation and properties of absorbable fibres from L-lactide copolymers. Polymer **34**, 942–951 (1993)
28. Leenslag, J., Pennings, A.: High-strength poly(L-lactide) fibres by a dry-spinning/hot-drawing process. Polymer **28**, 1695–1702 (1987)
29. Eling, B., Gogolewski, S., Pennings, A.: Biodegradable materials of poly(L-lactic acid): 1. Melt-spun and solution-spun fibres. Polymer. **23**, 1587–1593 (1982)
30. Yuan, X., Mak, A.F., Kwok, K., Yung, B.K., Yao, K.: Characterization of poly(L-lactic acid)fibers produced by melt spinning. J. Appl. Polym. Sci. **81**, 251–260 (2001)
31. Cicero, J.A., Dorgan, J.R.: Physical properties and fiber morphology of poly(lactic acid) obtained from continuous two-step melt spinning. J. Polym. Environ. **9**, 1–10 (2001)
32. Sawai, D., Yokoyama, T., Kanamoto, T., Sungil, M., Hyon, S.H., Myasnikova, L.P.: Crystal transformation and development of tensile properties upon drawing of poly(L-lactic acid) by solid-state coextrusion: effects of molecular weight. Macromol. Symp. **242**, 93–103 (2001)
33. Goutianos, S., Van der Schueren, L., Beauson, J.: Failure mechanisms in unidirectional self-reinforced biobased composites based on high stiffness PLA fibres. Compos. A Appl. Sci. Manuf. **117**, 169–179 (2019)
34. Beauson, J., Schillani, G., Van der Schueren, L., Goutianos, S.: The effect of processing conditions and polymer crystallinity on the mechanical properties of unidirectional self-reinforced PLA composites. Compos. A Appl. Sci. Manuf. **152**, 106668 (2022)
35. D1577-07.: Standard test methods for linear density of textile fibers. 100 Barr Harbor Drive, West Conshohocken, PA, USA: ASTM International (2018)
36. Weibull, W.: A statistical distribution function of wide applicability. ASME Journal of Applied Mechanics. **18**, 293–297 (1951)
37. Andersons, J., Joffe, R., Hojo, M., Ochiai, S.: Glass fibre strength distribution determined by common experimental methods. Compos. Sci. Technol. **62**, 131–145 (2002)
38. Thomason, J.L.: On the application of Weibull analysis to experimentally determined single fibre strength distributions. Compos. Sci. Technol. **77**, 74–80 (2013)
39. Revol, B.P., Thomassey, M., Ruch, F., Nardin, M.: Influence of the sample number for the prediction of the tensile strength of high tenacity viscose fibres using a two parameters Weibull distribution. Compos. Sci. Technol. **23**, 2701–2713 (2016)

40. Trustrum, K., Jayatilaka, A.D.S.: On estimating the Weibull modulus for a brittle material. J. Mater. Sci. **14**, 1080–1084 (1979)
41. El Asloun, M., Donnet, J.B., Guilpain, G., Nardin, M., Schultz, J.: On the estimation of the tensile strength of carbon fibres at short lengths. J. Mater. Sci. **24**, 3504–3510 (1989)
42. Bergman, B.: On the estimation of the Weibull modulus. J. Mater. Sci. Lett. **3**, 689–692 (1984)
43. Masson, J.J., Bourgain, E.: Some guidelines for a consistent use of the Weibuil statistics with ceramic fibres. Int. J. Fract. **55**, 303–319 (1992)
44. Liu, X., Dever, M., Fair, N., Benson, R.S.: Thermal and mechanical properties of Poly(lactic Acid) and Poly(ethylene/butylene Succinate) blends. J. Environ. Polym. Degrad. **5**(4), 225–235 (1997)
45. Sanchez-Garcia, M.D., Lagaron, J.M.: On the use of plant cellulose nanowhiskers to enhance the barrier properties of polylactic acid. Cellulose **17**, 987–1004 (2010)

Publisher's Note Springer Nature remains neutral with regard to jurisdictional claims in published maps and institutional affiliations.